SUPPORTING INFORMATION

for

Mono and dinuclear iridium(III) complexes featuring bis-tridentate coordination and Schiff-base bridging ligands: the beneficial effect of a second metal ion on luminescence efficiency

Emma V. Puttock, Amit Sil, Dmitry S. Yufit and J. A. Gareth Williams *

Department of Chemistry, Durham University, Durham, DH1 3LE, U.K.

** E-mail: j.a.g.williams@durham.ac.uk*

Synthesis and characterisation of H_2L^7

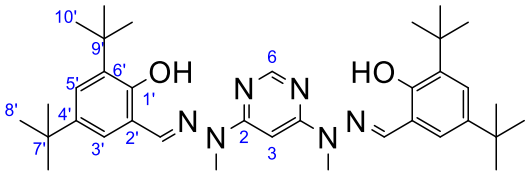

3,5-Di-tert-butyl-2-hydroxybenzaldehyde (84 mg, 0.36 mmol) was added slowly to a stirring solution of 4,6-di(1-methylhydrazino)pyrimidine (30 mg, 0.18 mmol) in MeOH (1 mL). The yellow solution was stirred under argon at reflux for 1 hour before cooling to ambient temperature. The resulting lemon slurry was filtered and washed with cold methanol to yield 68mg of a white powder (0.11 mmol, 61% yield). ^{1}H NMR ($CDCl_3$, 700 MHz): 11.50 (2H, s, H^{OH}), 8.54 (1H, s, H^3), 7.99 (2H, s, H^{imine}), 7.33 (2H, d, J = 2.5, $H^{5'}$), 7.11 (2H, d, J = 2.5, $H^{3'}$), 6.78 (1H, s, H^6), 3.67 (6H, s, H^{NMe}), 1.41 (18H, s, $H^{8'}$), 1.33 (18H, s, $H^{10'}$). ^{13}C NMR ($CDCl_3$, 176 MHz): 162.2 (C^2), 157.6 (C^6), 154.5 ($C^{1'}$), 143.6 (C^{imine}), 140.9 ($C^{4'}$), 136.8 ($C^{6'}$), 125.8 ($C^{5'}$), 125.5 ($C^{3'}$), 117.9 ($C^{2'}$), 86.2 (C^3), 35.3 ($C^{9'}$), 34.3 ($C^{7'}$), 31.7 ($C^{10'}$), 30.4 (C^{NMe}), 29.8 ($C^{8'}$). MS (ES+): *m/z* 601 $[M+H]^+$; HRMS (ES+): *m/z* 601.4253 $[M+H]^+$; calculated for $[C_{36}H_{53}N_6O_2]^+$ 601.4230.

Synthesis and characterisation of $[Ir(dpyx)HL^7]PF_6$

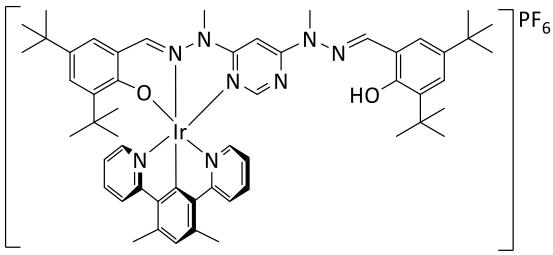

H_2L^7 (30 mg, 0.05 mmol) and $[Ir(dpyx)Cl(\mu\text{-}Cl)]_2$ (26 mg, 0.025 mmol) were heated to 195°C in ethylene glycol (1.5 mL) for 90 min under argon. The resulting slurry was allowed to cool to ambient temperature, then H_2O (5 mL) was added and an orange-brown solid isolated by filtration. This material was dissolved in the minimum volume of hot DMSO and added dropwise into a saturated aqueous solution of KPF_6. The resulting precipitate was separated by centrifugation and washed with H_2O to yield the yellow mononuclear complex (29 mg, 0.024 mmol, 48% yield).

^{1}H NMR (CD_3CN, 700 MHz): 11.37 (1H, s), 8.92 (1H, s), 8.20 (2H, d, J = 8), 8.16 (1H, s), 7.82 – 7.78 (4H, m), 7.55 (1H, d, J = 2.5), 7.42 (1H, d, J = 2), 7.32 (1H, d, J = 2), 7.22 (1H, d, J = 3), 7.15 (1H, s), 7.11 (1H, s), 7.04 (2H, ddd, J = 7, 5 and 1), 6.58 (1H, s), 4.10 (3H, s), 3.48 (3H, s), 1.49 (9H, s), 1.30 (18H, s), 0.70 (9H, s). ^{13}C NMR (CD_3CN, 176 MHz): 171.2, 159.9, 159.6, 159.4, 158.9, 155.3, 151.4, 142.6, 141.8, 141.6, 140.4, 139.3, 139.2, 137.6, 137.3, 132.3, 130.1, 128.6, 127.5, 127.3, 124.6, 123.5, 119.3, 118.7, 118.3, 84.8, 35.9, 35.8, 34.9, 34.6, 33.6, 31.7, 31.7, 30.6, 29.8, 29.2, 22.5. MS (ES+): *m/z* 1052 $[M+H]^+$; HRMS (ES+): *m/z* 1049.4940 $[M]^+$; calculated for $[C_{54}H_{66}N_8O_2Ir]^+$ 1049.4915.

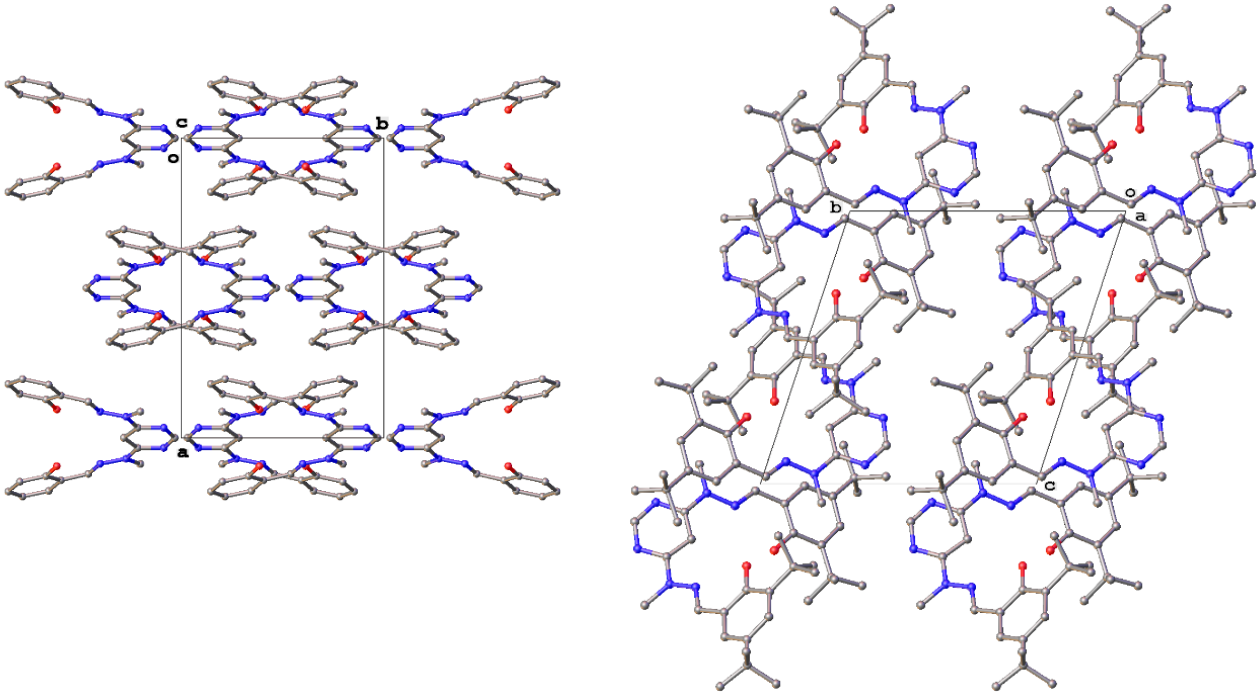

Figure S1 *Crystal packing in the ditopic proligands H_2L^5 (left) and H_2L^7 (right). Hydrogen atoms are omitted for clarity.*

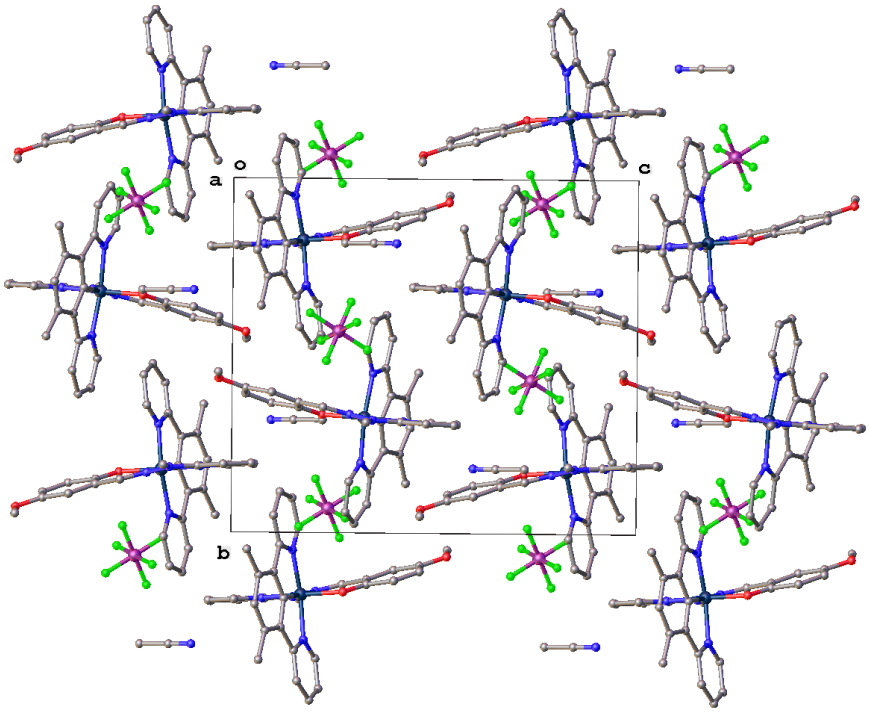

Figure S2 *Crystal packing for the complex $[Ir(dpyx)L^4]PF_6$, with H atoms omitted for clarity.*

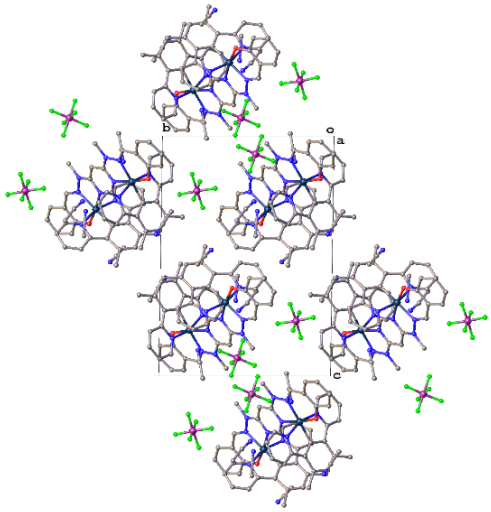

Figure S3 *Crystal packing for [{Ir(dpyx)$_2$}L^5](PF$_6$)$_2$, with H atoms omitted for clarity.*

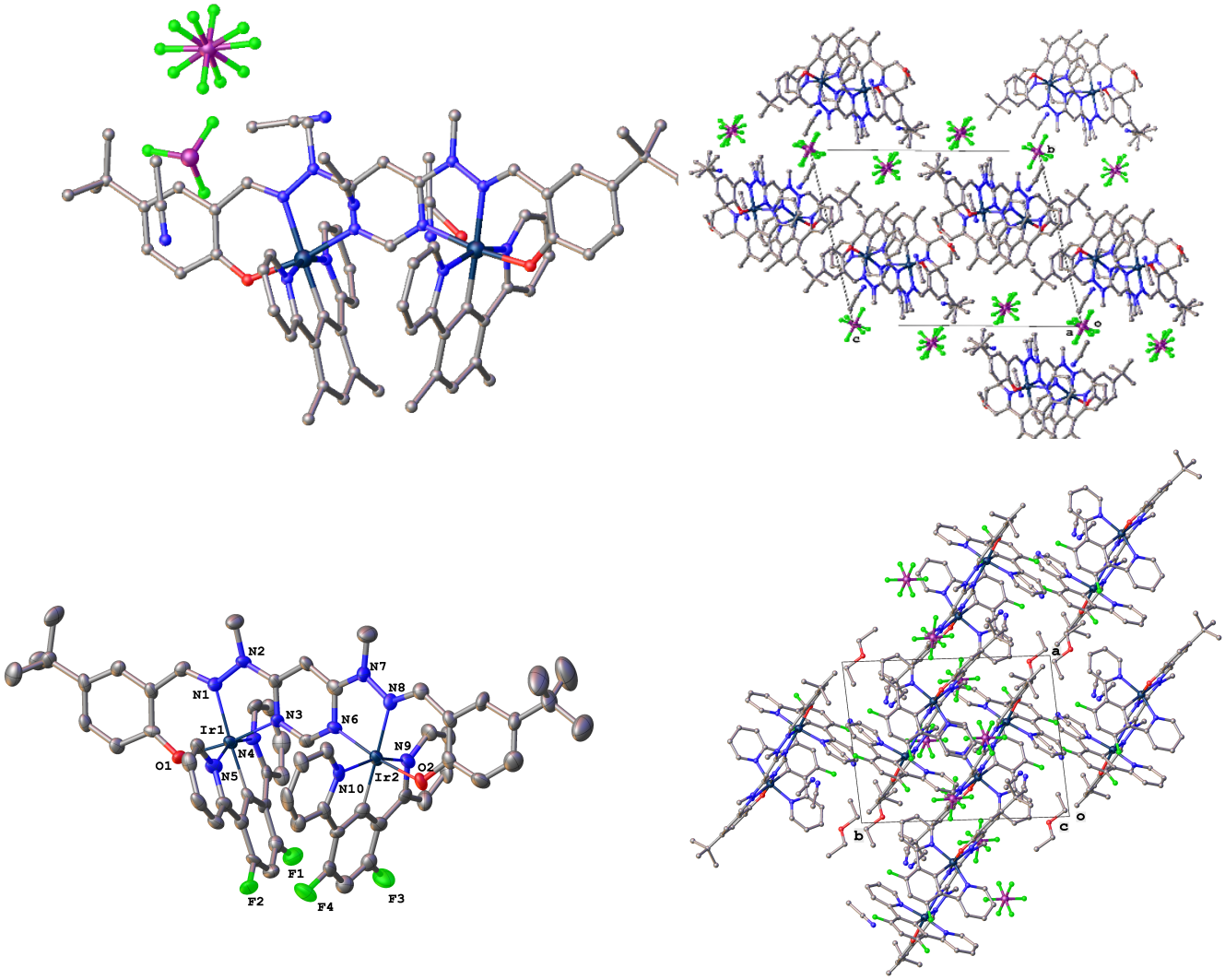

Figure S4 *The molecular structure (left) and crystal packing (right) of the dinuclear complexes [{Ir(dpyx)$_2$}L^6](PF$_6$)$_2$ (top) and [{Ir(dpyF)$_2$}L^6](PF$_6$)$_2$ (bottom); hydrogen atoms omitted for clarity.*

Table S1 Selected bond lengths and angles in the mono- and dinuclear iridium(III) complexes, determined by X-ray diffraction analysis of crystals at 120 K.

Bond lengths (Å) and angles (°) [(a)]	**$[Ir(dpyx)L^4]^+$**	**$[\{Ir(dpyx)_2\}L^5]^{2+}$**	**$[\{Ir(dpyx)_2\}L^6]^{2+}$**	**$[\{Ir(dpyF)_2\}L^6]^{2+}$**
Ir1–C	1.948(2)	1.971(10)	1.952(5)	1.945(9)
Ir1–N(hyd)	2.078(1)	2.066(8)	2.079(5)	2.076(7)
Ir1–N(py[m]^{NNO})	2.019(1)	2.017(7)	2.027(5)	2.025(7)
Ir1–N4(py^{NCN})	2.035(1)	2.049(9)	2.045(5)	2.057(7)
Ir1–N5(py^{NCN})	2.053(1)	2.023(8)	2.051(5)	2.051(8)
Ir1–O	2.033(1)	2.013(7)	2.026(4)	2.024(6)
Ir2–C		1.966(9)	1.947(5)	1.945(9)
Ir2–N(hyd)		2.074(7)	2.079(5)	2.068(7)
Ir2–N(pym)		2.007(8)	2.029(5)	1.997(7)
Ir2–N9(py^{NCN})		2.051(8)	2.053(5)	2.021(8)
Ir2–N10(py^{NCN})		2.073(8)	2.055(5)	2.057(7)
Ir2–O		2.036(7)	2.029(4)	2.008(6)
N4-Ir1-N5	161.42(6)	161.3(4)	160.9(2)	159.2(3)
N(pym)-Ir1-O	171.70(5)	172.1(3)	171.6(2)	171.6(3)
N(hyd)-Ir1-C	175.57(6)	177.7(4)	176.0(2)	177.0(3)
N9-Ir2-N10		161.2(3)	160.4(2)	161.2(3)
N(pym)-Ir2-O		171.5(3)	171.4(2)	172.0(3)
N(hyd)-Ir2-C		176.2(3)	178.2(2)	178.6(3)
Ir1···Ir2	8.804 [(b)]	5.984 [(c)]	6.021 [(c)]	5.943 [(c)]

(a) N(hyd) = hydrazone nitrogen; N(pym) = pyrimidine nitrogen; N(py[m]^{NNO}) = nitrogen of the pyridine ring of the *N^N^O* ligand for $[Ir(dpyx)L^4]^+$ and nitrogen of the pyrimidine ring bonded to Ir1 for the dinuclear complexes. *(b)* Intermolecular Ir···Ir distance. *(c)* Intramolecular Ir···Ir distance.

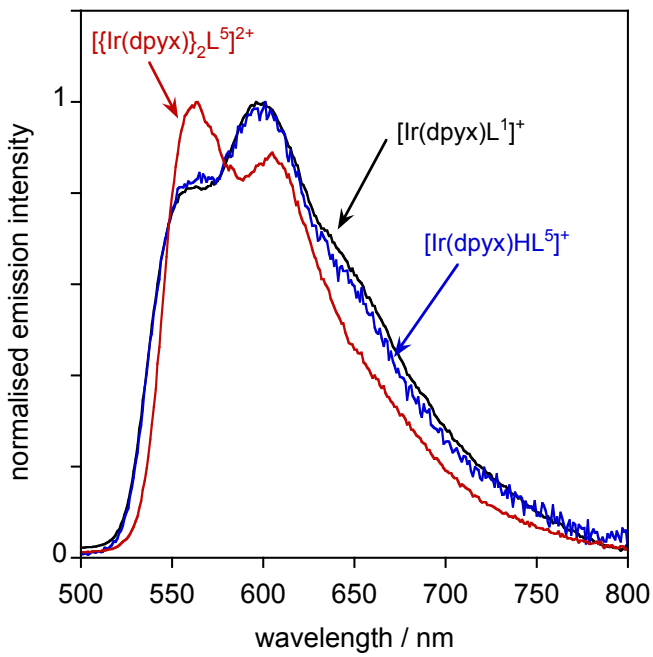

Figure S5 *Comparison of the emission spectra of the mononuclear complexes $[Ir(dpyx)L^1]PF_6$ and $[Ir(dpyx)HL^5]PF_6$ with that of dinuclear $[\{Ir(dpyx)\}_2L^5](PF_6)_2$ in CH_2Cl_2 at 295 K, showing the 0,1 vibrational component to be more intense than the 0,0 for the mononuclear complexes and vice versa for the dinuclear complex.*

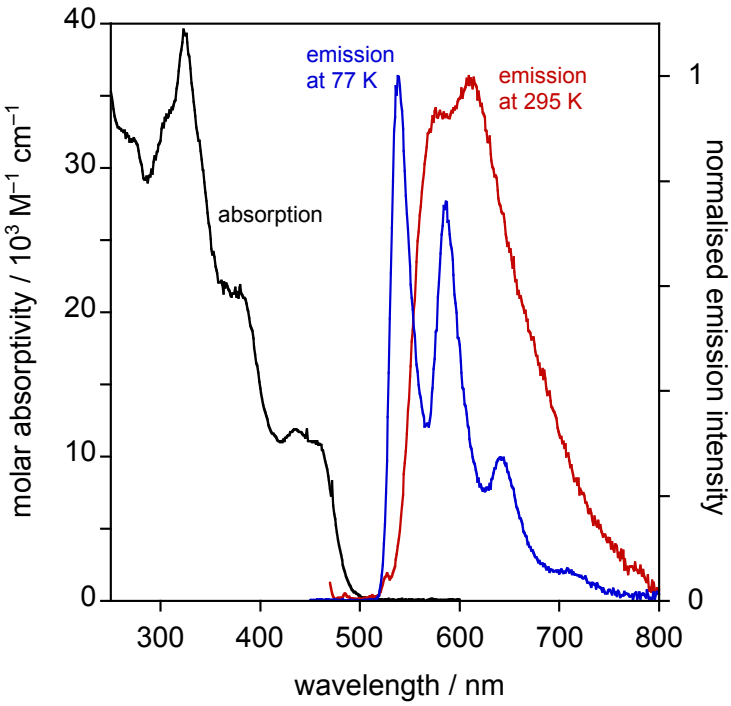

Figure S6 *Absorption and emission spectra of $[Ir(dpyx)HL^7]PF_6$ in CH_2Cl_2 at 295 K (black and red lines respectively) and the emission spectrum in EPA at 77 K (blue line).*

NMR Spectra

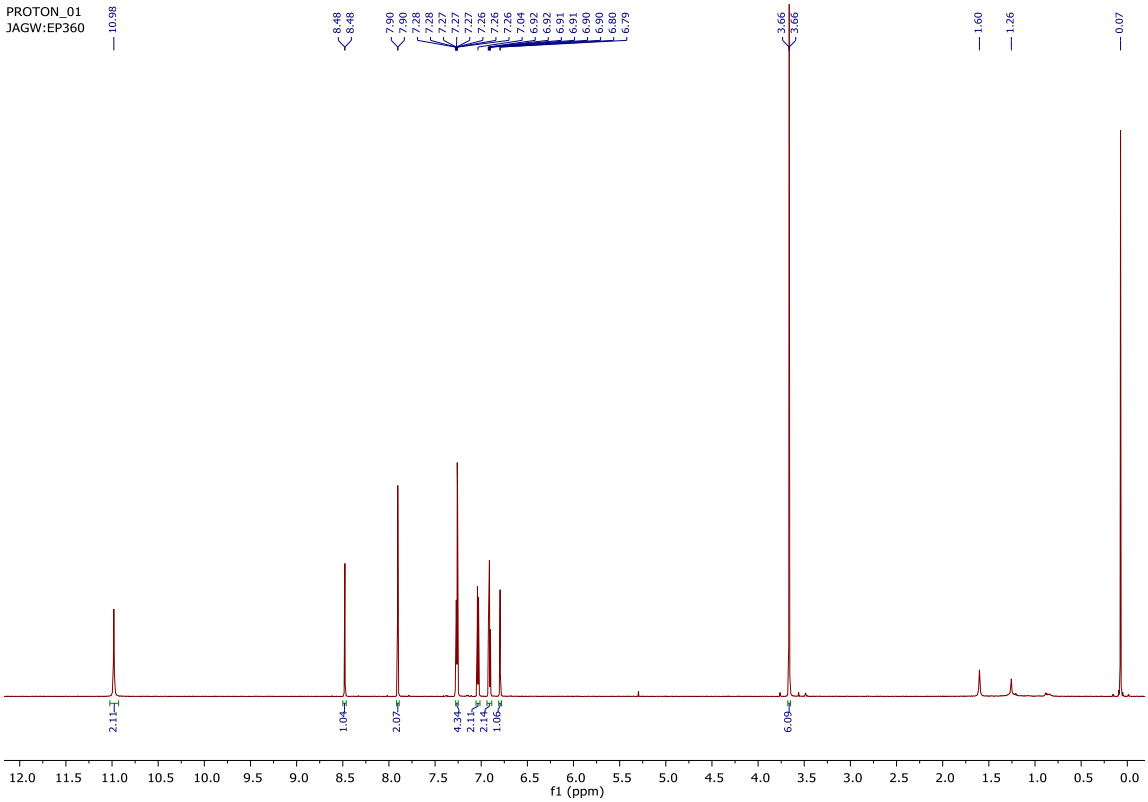

Figure S7 ^{1}H NMR (700 MHz, $CDCl_3$) spectrum of $\mathbf{H_2L^5}$.

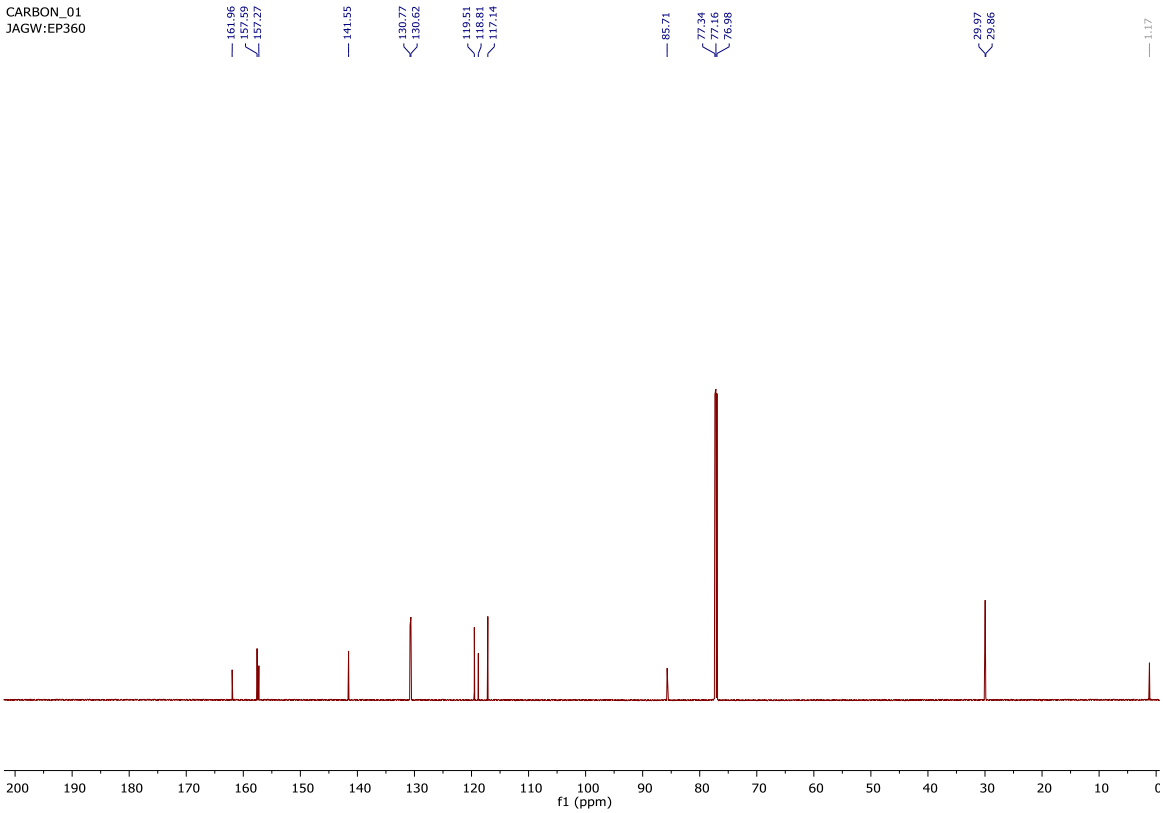

Figure S8 ^{13}C NMR (176 MHz, $CDCl_3$) spectrum of $\mathbf{H_2L^5}$.

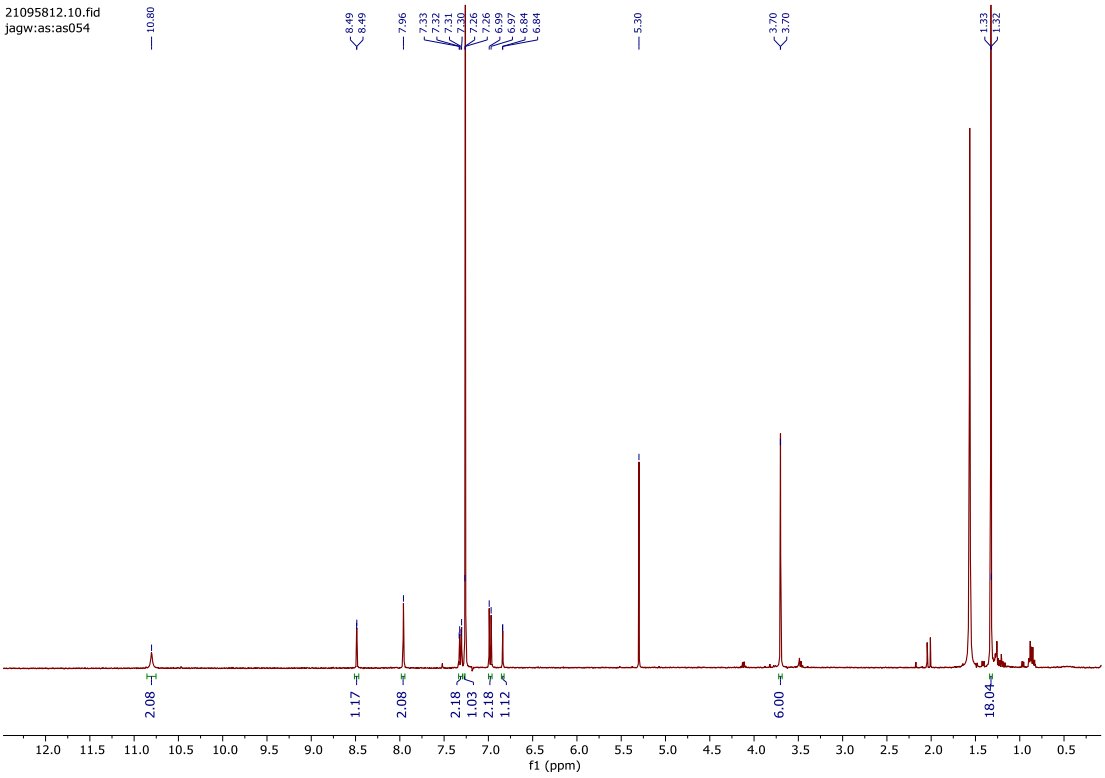

Figure S9 ^{1}H NMR (700 MHz, $CDCl_3$) spectrum of $\mathbf{H_2L^6}$.

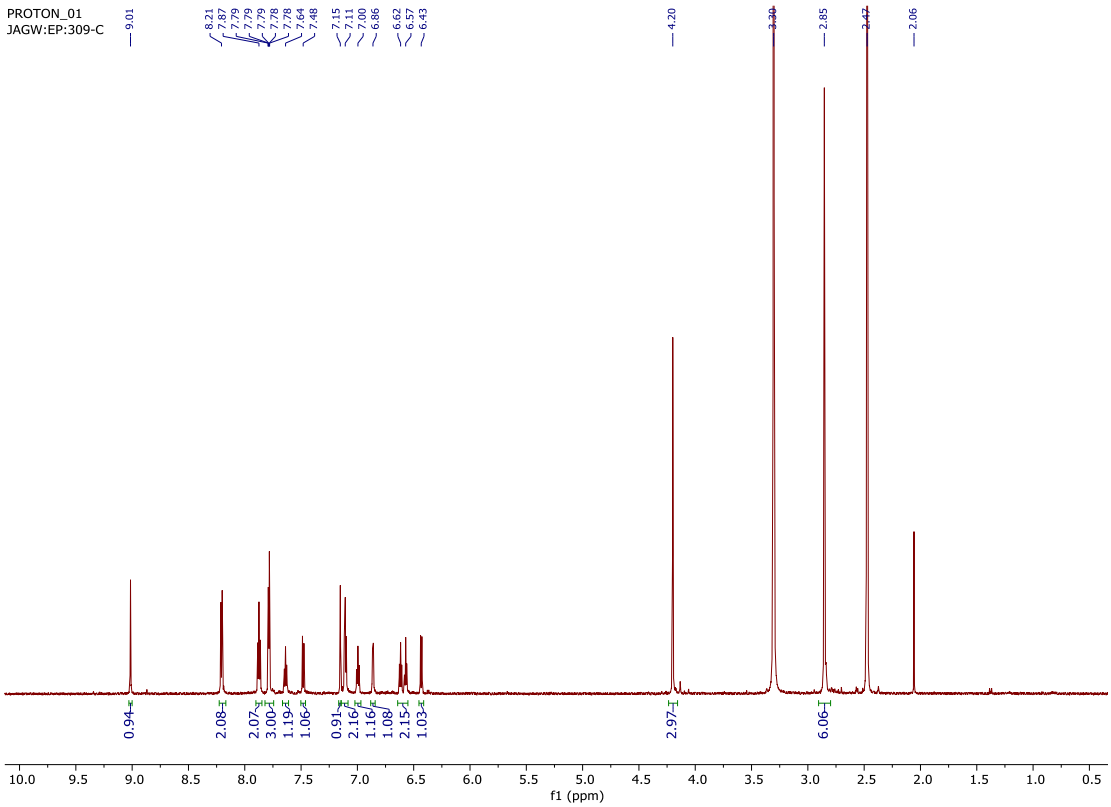

Figure S10 ^{1}H NMR (700 MHz, DMSO-d6) spectrum of $\mathbf{[Ir(dpyx)L^1]PF_6}$.

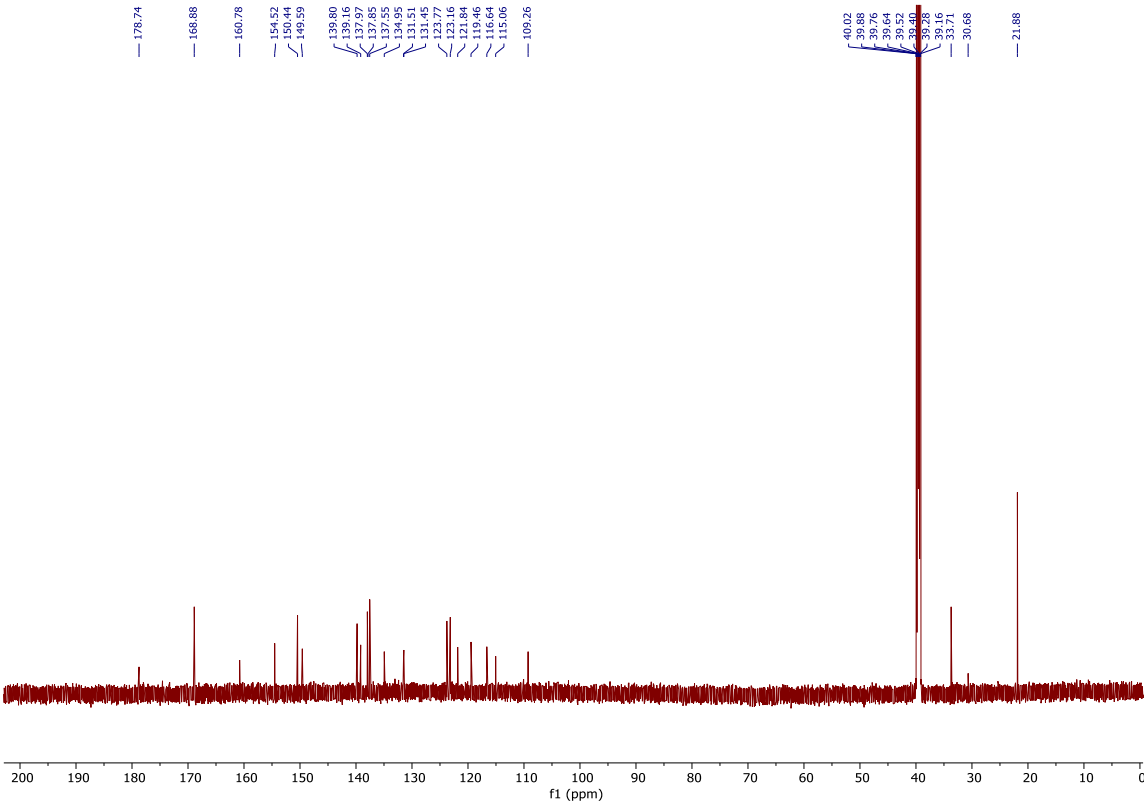

Figure S11 ^{13}C NMR (176 MHz, DMSO-d6) spectrum of **[Ir(dpyx)L^1]PF$_6$**.

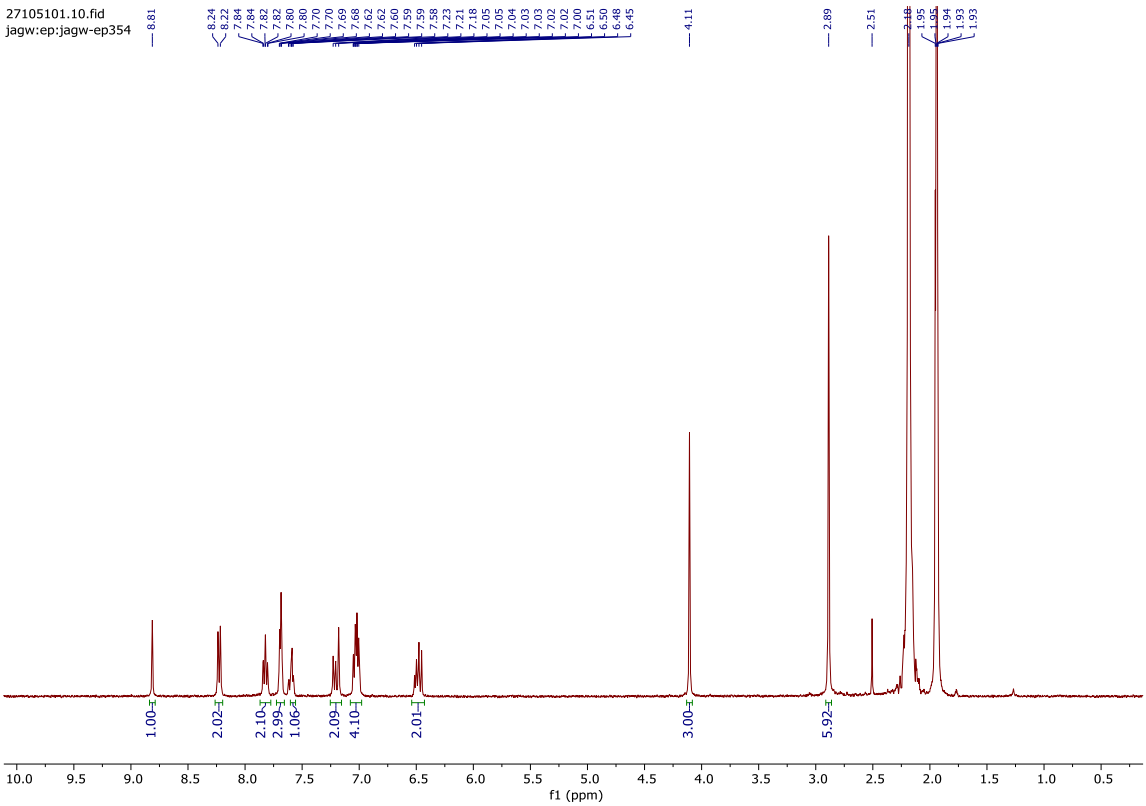

Figure S12 ^{1}H NMR (700 MHz, CD_3CN) spectrum of **[Ir(dpyx)L^2]PF$_6$**.

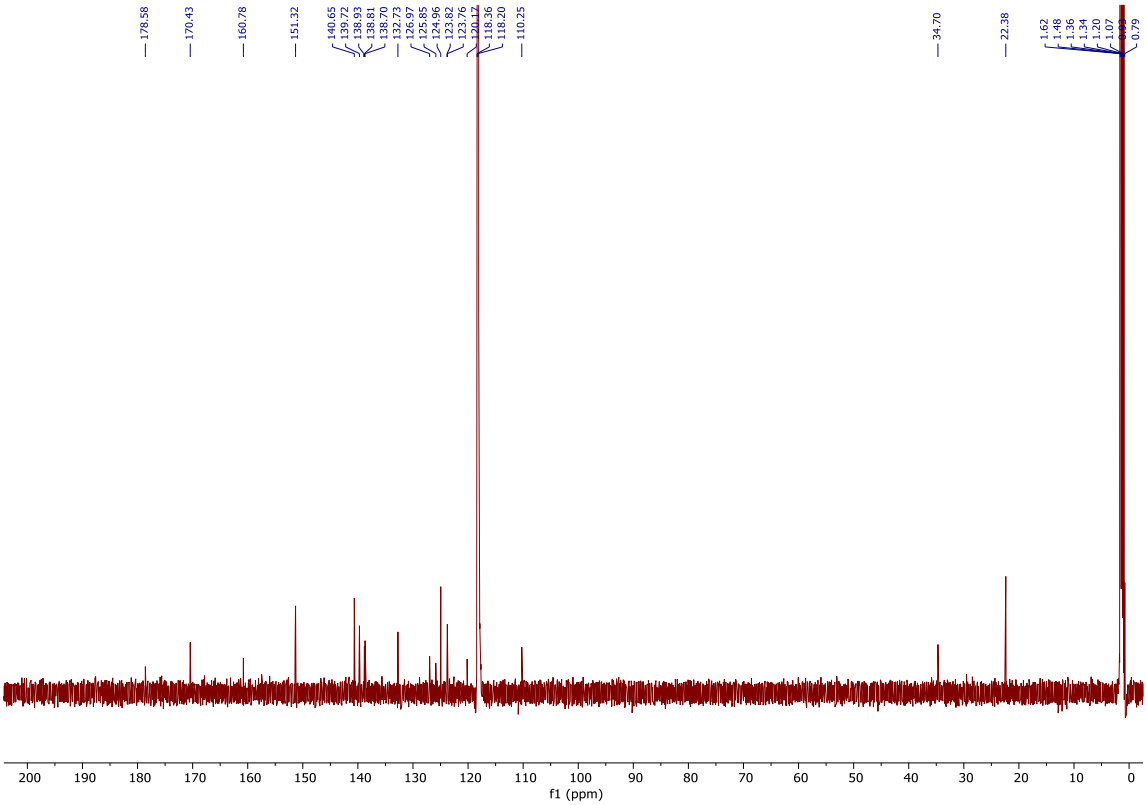

Figure S13 ^{13}C NMR (176 MHz, CD_3CN) spectrum of **[Ir(dpyx)L^2]PF$_6$**.

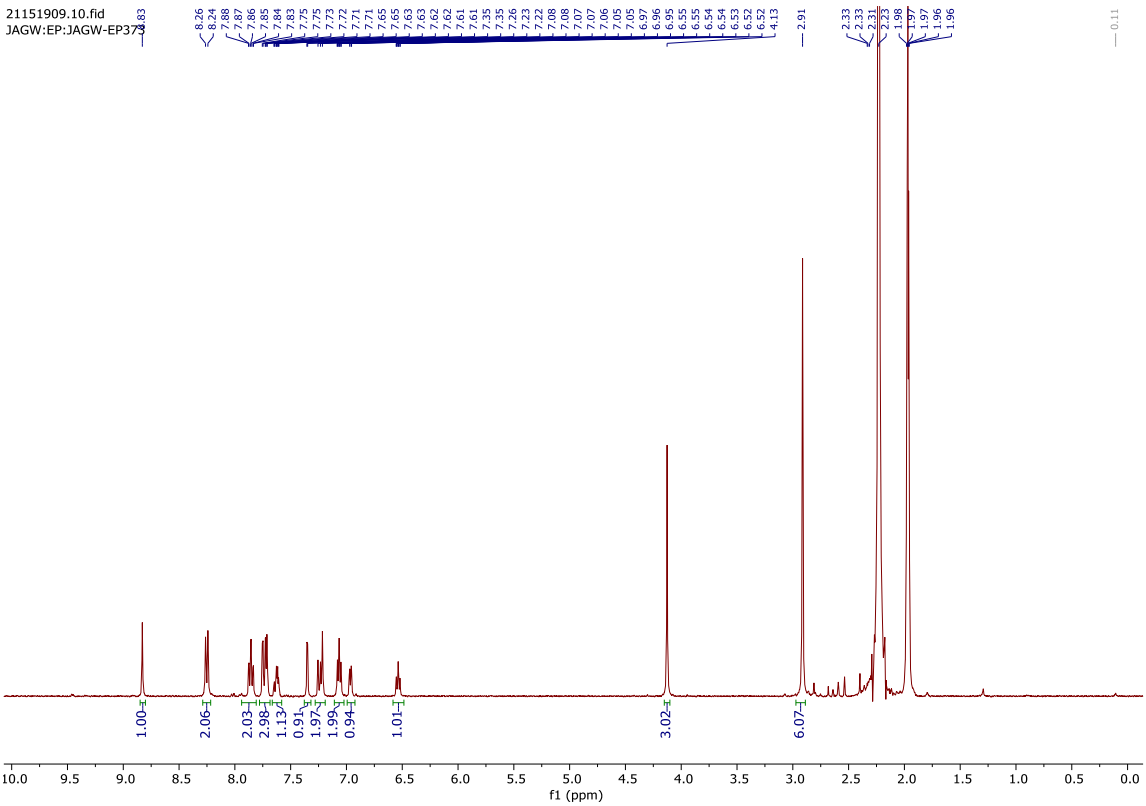

Figure S14 ^{1}H NMR (700 MHz, CD_3CN) spectrum of **[Ir(dpyx)L^3]PF$_6$**.

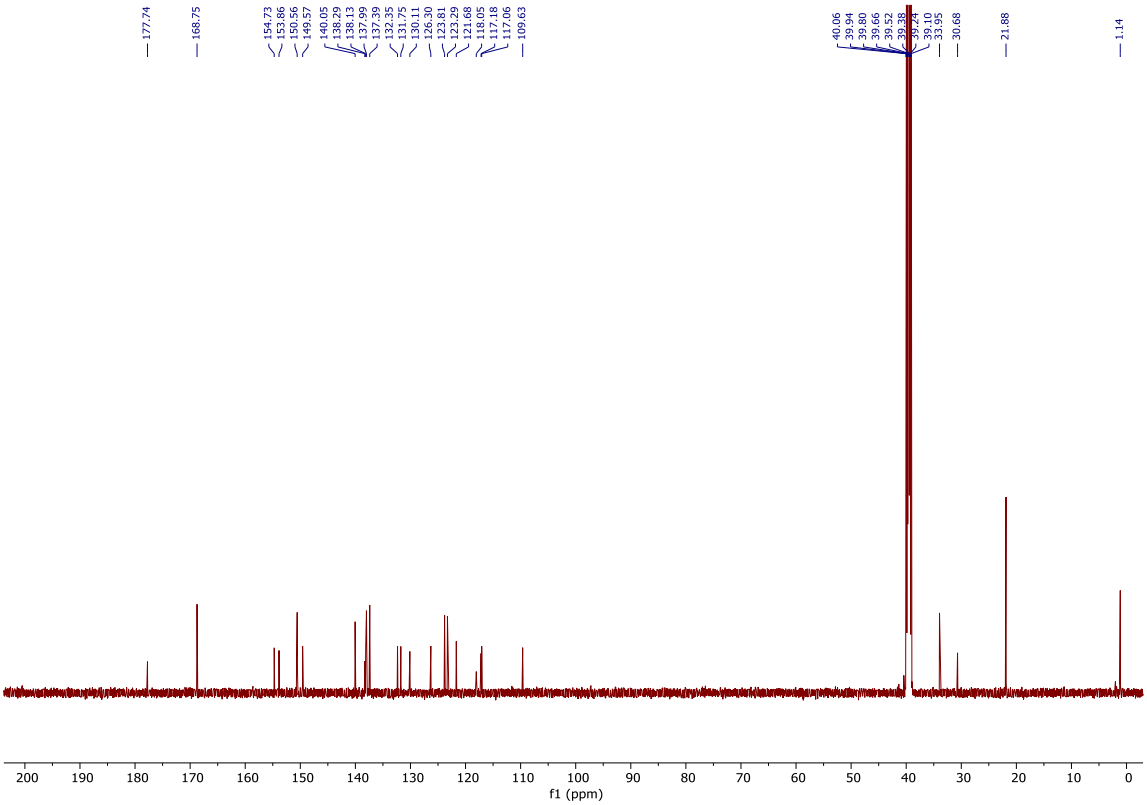

Figure S15 ^{13}C NMR (176 MHz, CD_3CN) spectrum of **[Ir(dpyx)L^3]PF$_6$**.

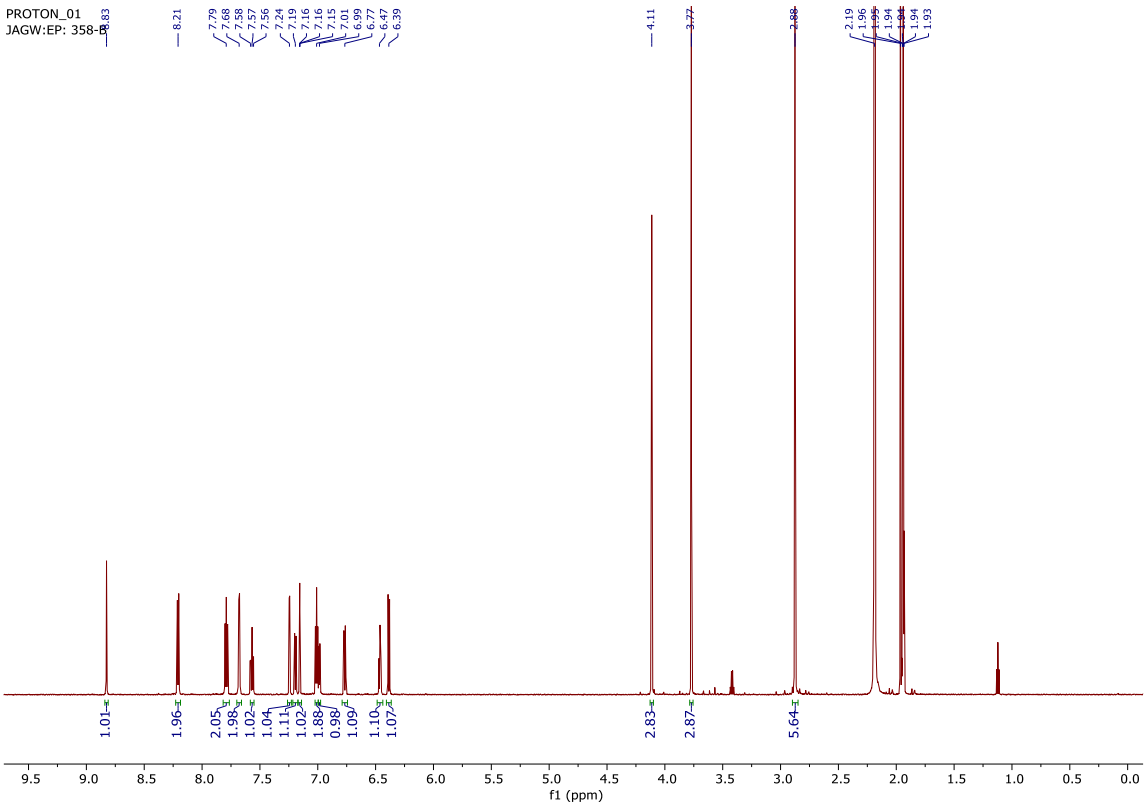

Figure S16 ^{1}H NMR (700 MHz, CD_3CN) spectrum of **[Ir(dpyx)L^4]PF$_6$**.

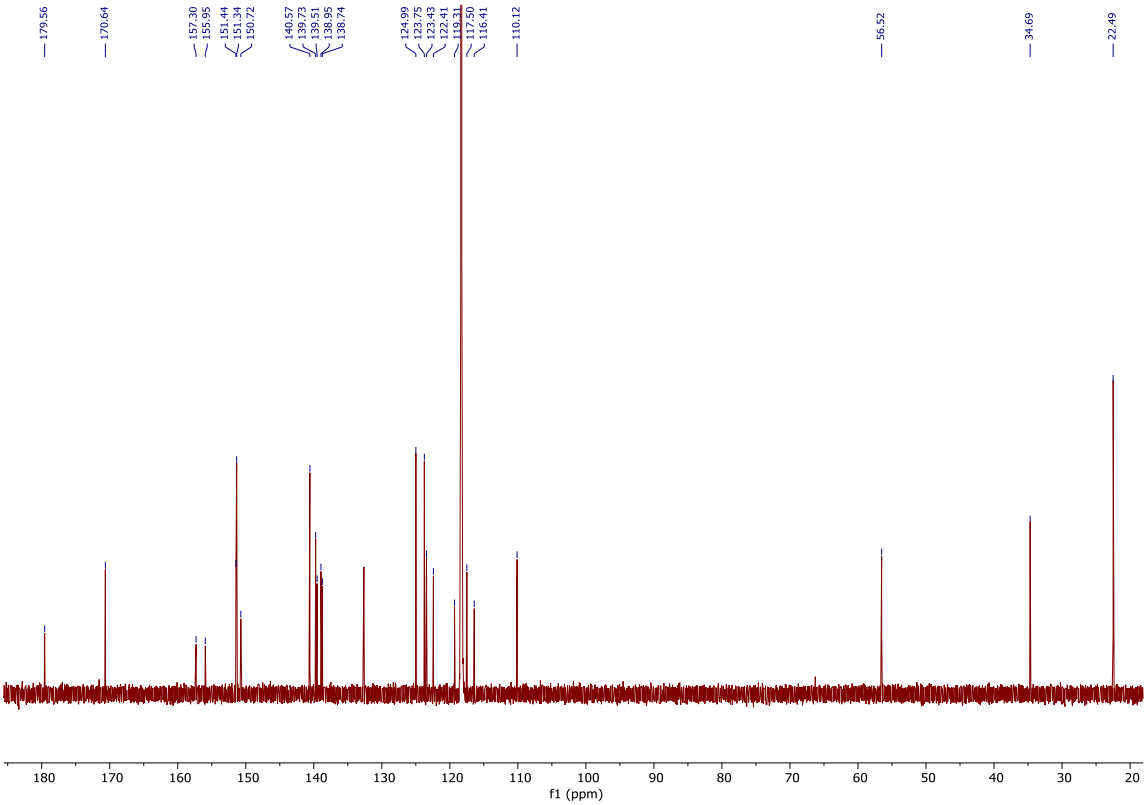

Figure S17 ^{13}C NMR (176 MHz, CD_3CN) spectrum of **[Ir(dpyx)L^4]PF$_6$**.

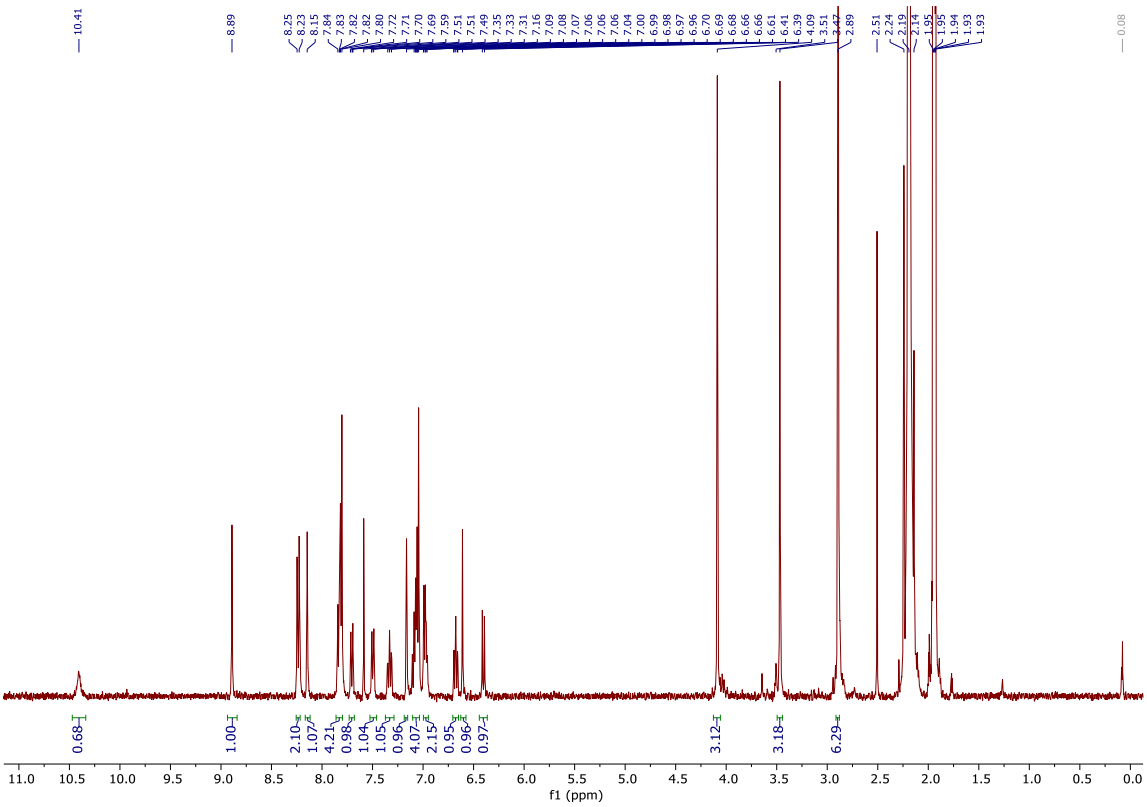

Figure S18 ^{1}H NMR (700 MHz, CD_3CN) spectrum of **[Ir(dpyx)HL^5]PF$_6$**.

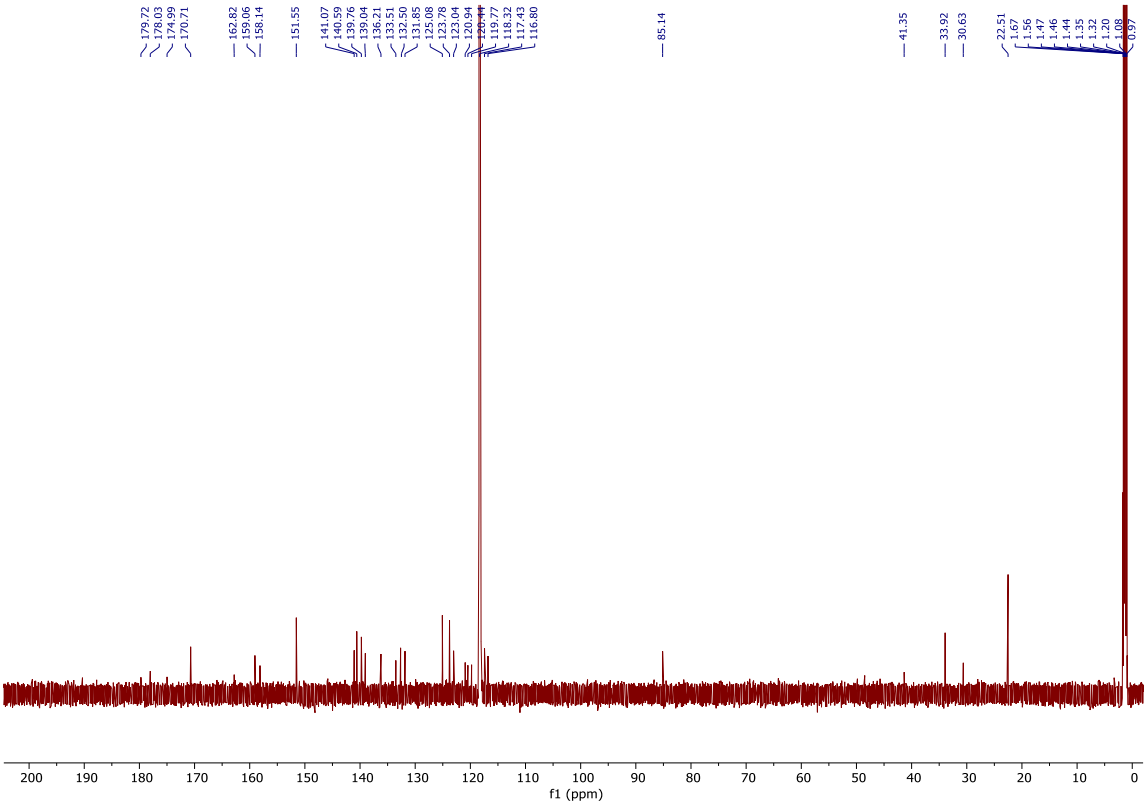

Figure S19 ^{13}C NMR (176 MHz, CD_3CN) spectrum of **[Ir(dpyx)HL^5]PF$_6$**.

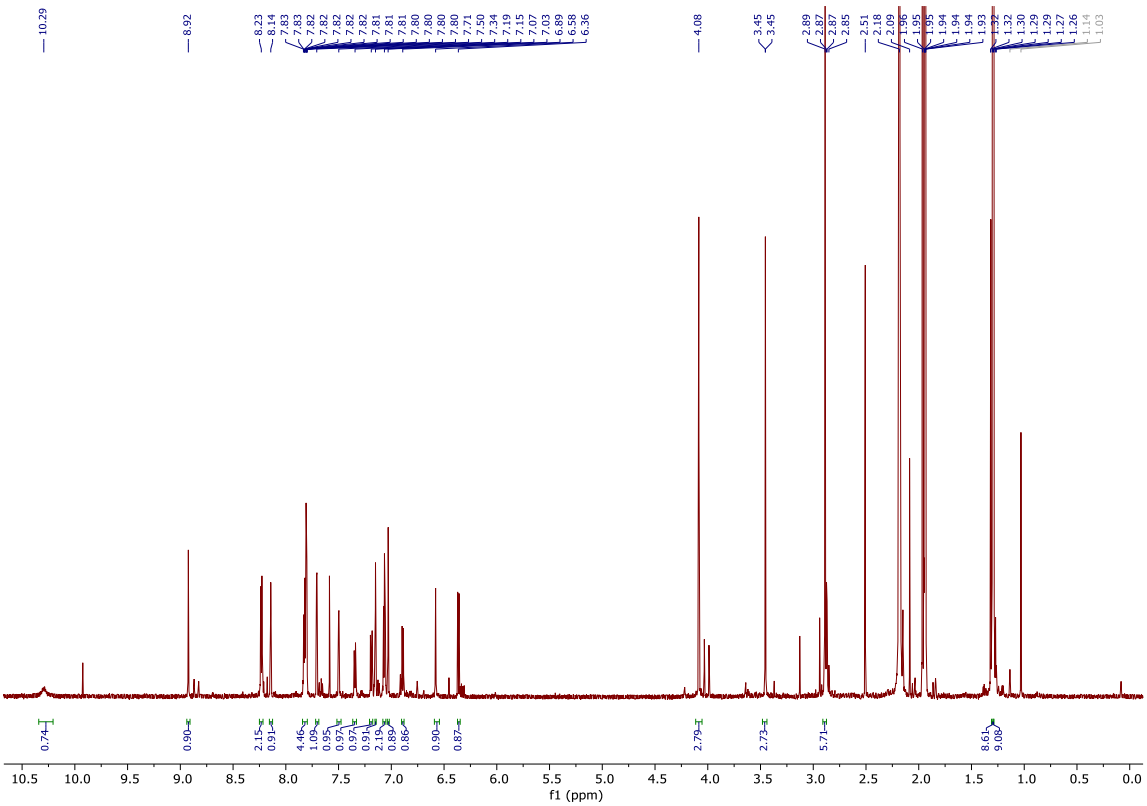

Figure S20 ^{1}H NMR (700 MHz, CD_3CN) spectrum of **[Ir(dpyx)HL^6]PF$_6$**.

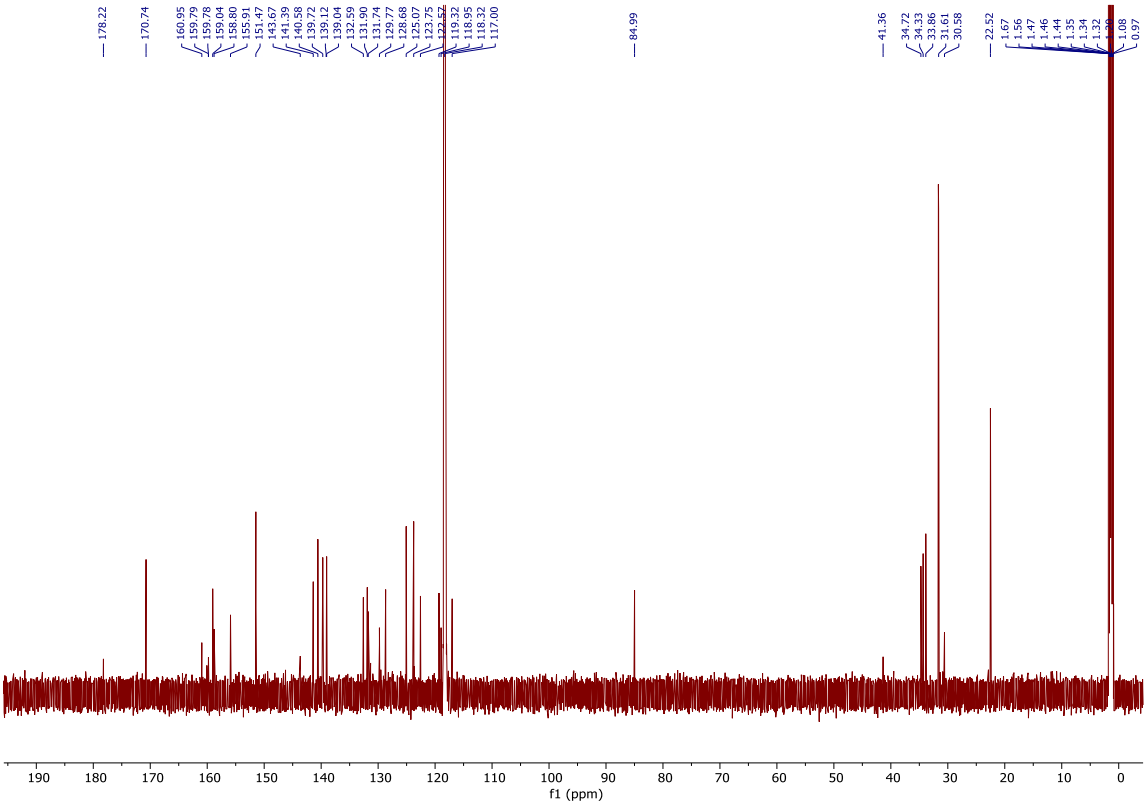

Figure S21 ^{13}C NMR (176 MHz, CD_3CN) spectrum of **[Ir(dpyx)HL^6]PF$_6$**.

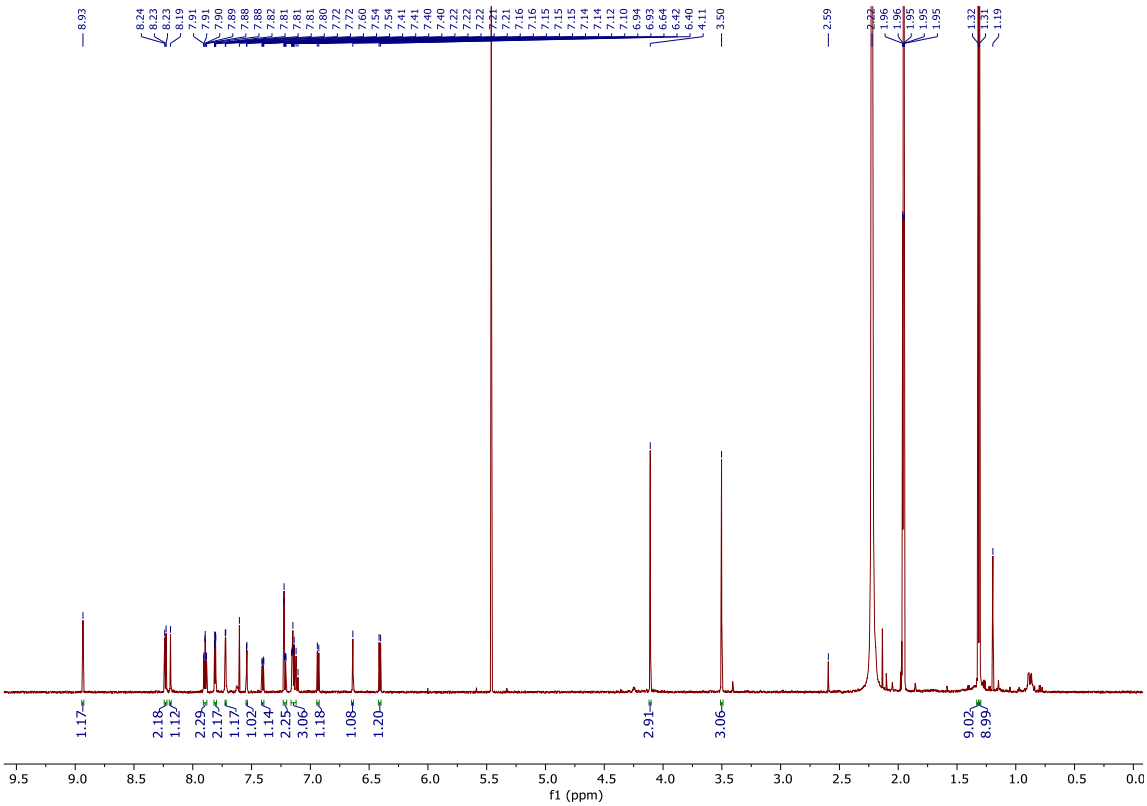

Figure S22 ^{1}H NMR (700 MHz, CD_3CN) spectrum of **[Ir(dpyF)HL^6]PF$_6$**.

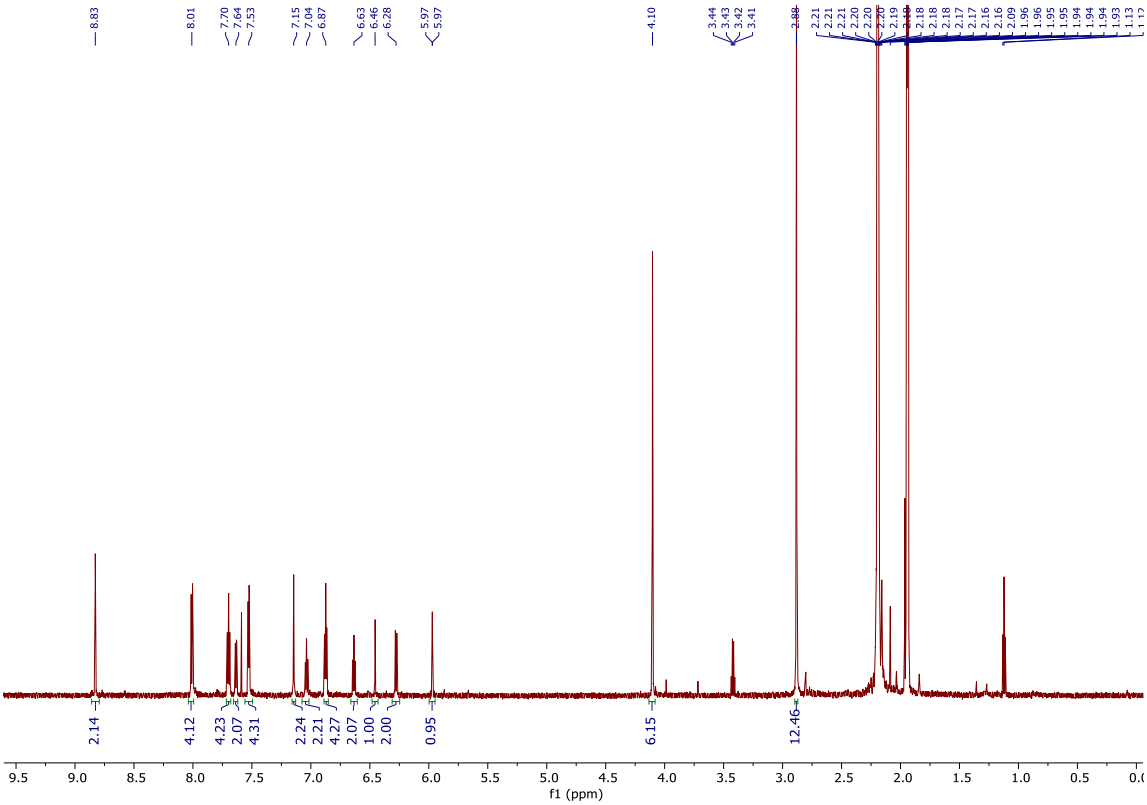

Figure S23 ^{1}H NMR (700 MHz, CD_3CN) spectrum of **[{Ir(dpyx)}$_2$L^5](PF$_6$)$_2$**.

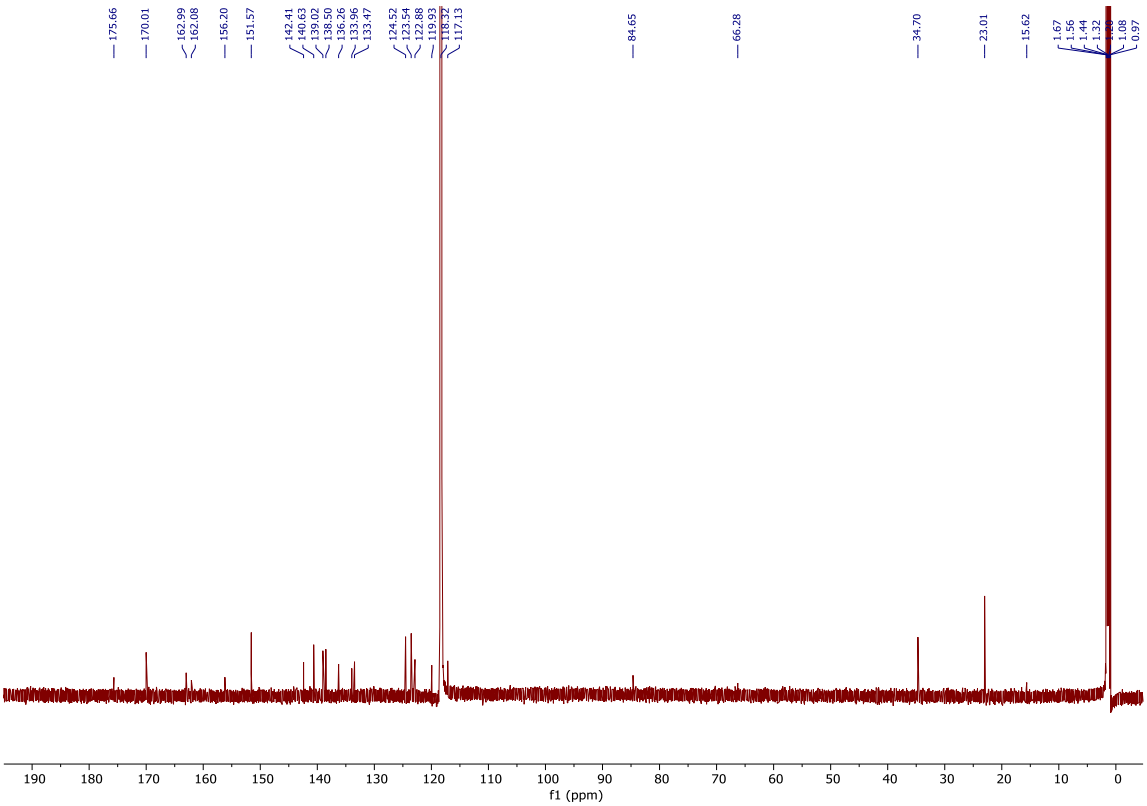

Figure S24 ^{13}C NMR (176 MHz, CD_3CN) spectrum of **[{Ir(dpyx)}$_2$L^5](PF$_6$)$_2$**.

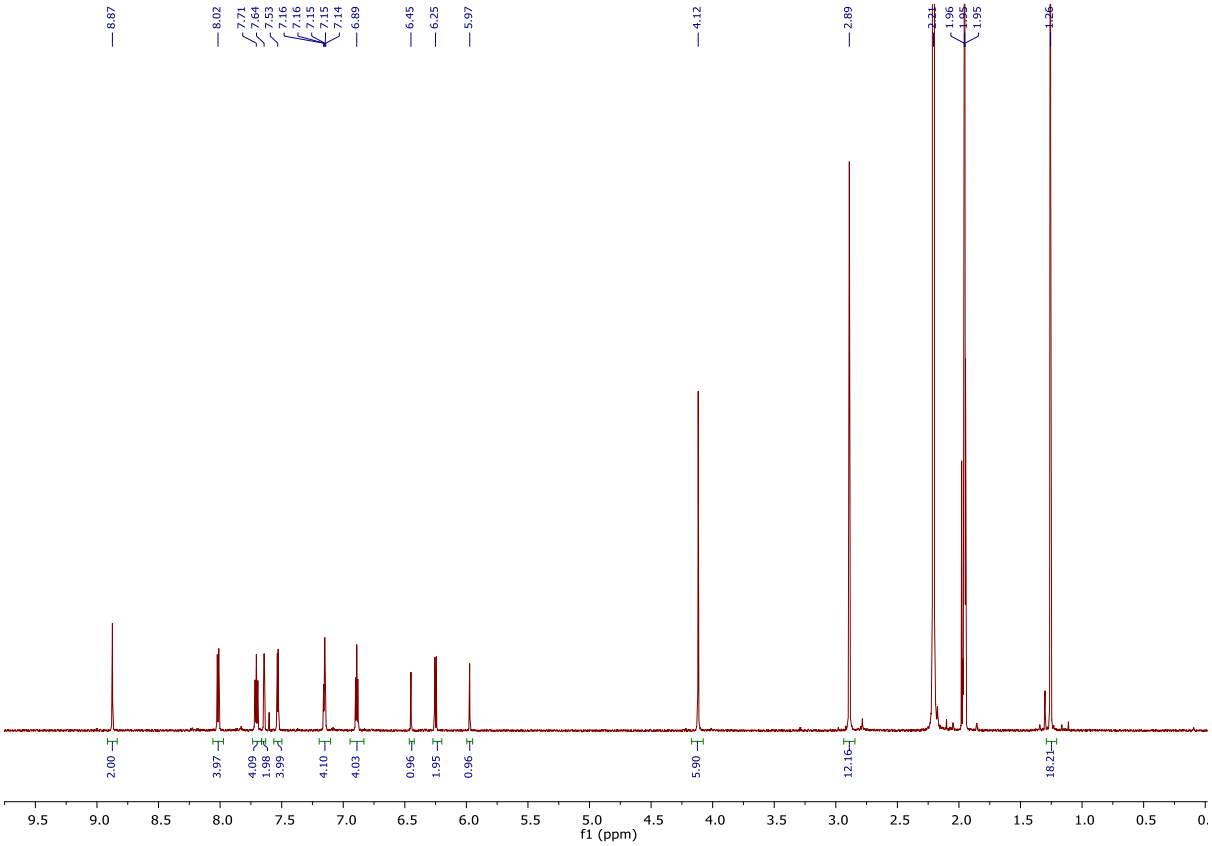

Figure S25 ^{1}H NMR (700 MHz, CD_3CN) spectrum of **[{Ir(dpyx)}$_2$L^6](PF$_6$)$_2$**.

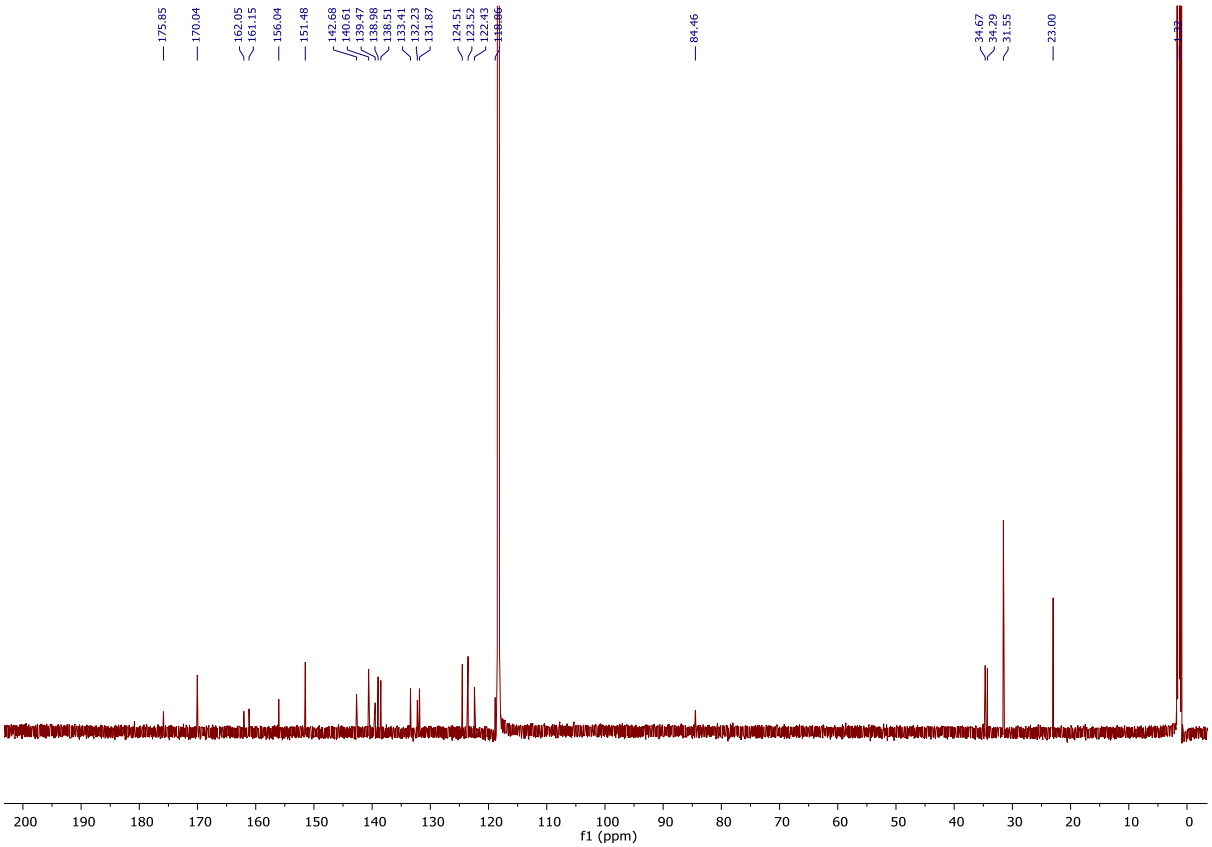

Figure S26 ^{13}C NMR (176 MHz, CD_3CN) spectrum of **[{Ir(dpyx)}$_2$L^6](PF$_6$)$_2$**.

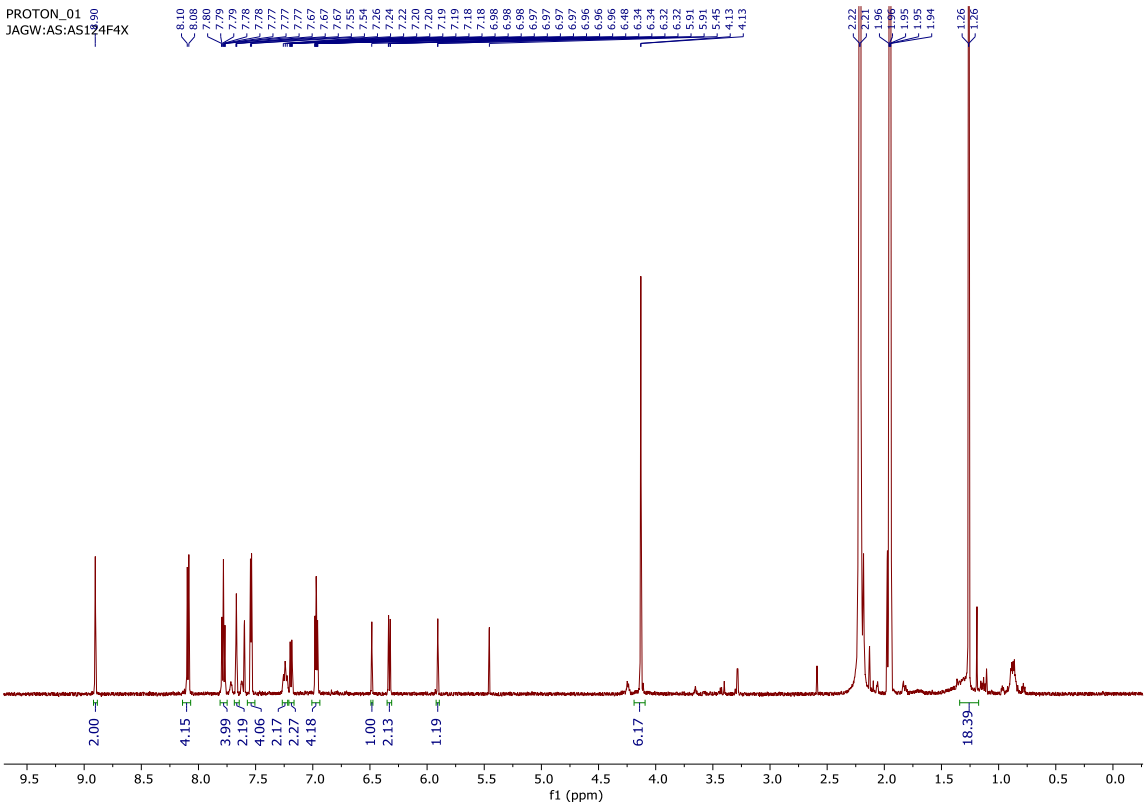

Figure S27 ^{1}H NMR (700 MHz, CD_3CN) spectrum of **[{Ir(dpyF)}$_2$L^6](PF$_6$)$_2$.**